MODEL OF ELECTROMAGNETIC WAVE SCATTERING FROM SEA SURFACE WITH AND WITHOUT OIL SLICKS

A. I. Timchenko

Institute of Radio Physics and Electronics, NASU
12 Acad. Proskura St., 61085 Kharkov, Ukraine

A. E. Serebryannikov

Institute of Radio Astronomy, NASU
4 Chervonopraporna St., 61002 Kharkov, Ukraine

K. F. Schuenemann

AB Hochfrequenztechnik
Technische Universitaet Hamburg-Harburg
D-21071 Hamburg, Germany

Abstract—The problem of scattering from sea surface covered by oil films is investigated by using a composite random rough surface model. A model is developed which extends the range of validity beyond the small perturbation theory. A general expression for the scattering cross section is obtained taking into account a modulation of the rough surface by long surface waves. A numerical study for the radar scattering cross section is provided in order to investigate the influence of the different ranges of the rough surface spectrum on the backscattering depression. For the case of backscattering, the contrast of radar signals scattered from a slick-free and a slick-covered surface is evaluated. The study is also carried through for two-frequency probing. A possibility to explain the mechanism of the depression of backscattering is discussed. The results of this study demonstrate the importance of the improved model which takes into account the entire spectrum of the sea surface roughness for the description of scattering from an ocean surface with and without oil slicks.

1. INTRODUCTION

The ability to detect and monitor oil spills at sea is becoming increasingly important, because of the threats posed by such pollution to marine operations and wildlife [1, 2]. In recent years, remote-sensing techniques and corresponding processing techniques have been developed for this purpose. In Refs. [3, 4], semiautomatic systems for oil spill detection have been suggested and examined. These systems are aiming on an automatic identification of oil spots with high probability. The methods are based on a combination of prior knowledge, Gaussian densities, and rule-based density corrections. An incorporation of a well-developed theoretical model which adequately describes the behavior of the signal scattered from oil spot and sea surface should result in a further increase of the accuracy of the automatic detection methods. Such a model must describe the scattering from a rough surface with a broad spectrum of roughness.

It was shown that oil films when spread on the surface of rough seas damp the surface waves. This damping causes a reduction in the amount of radar backscatter observed at intermediate incidence angles, and provides the physical basis for the use of remote sensing (radar) to detect oil spills on sea. The observed reduction, as was suggested in [5], may be explained in terms of a resonant-type damping of short gravity waves, with non-linear wave-wave interaction transferring energy from longer waves to the energy sink in the short-wave region. Thus oil films on sea lead to a suppression of the backscattered signal over all the ranges of the surface wave spectrum.

For a correct interpretation of the change of the radar backscatter from sea surface with and without oil films it is necessary to take into account scattering from a rough surface with a broad spectrum of roughness. However, most measurements of the radar backscatter from slicks have been interpreted in terms of the small perturbation theory (see, for example, [5]). As a result, the experimental observations not always agree with the theoretical conclusions [2].

Several attempts have been made to improve the scattering model. Most often, two practical limits are considered. These are the small

perturbation model (SPM) and the Kirchhoff approximation (KA). For surfaces showing small values of the root mean square (rms) height and slope, SPM is the most commonly used formalism [6–8]. If the irregularities of the surface show relatively small slopes and large curvature radii, KA in a geometrical optics variant can be used [9]. In the past two decades, many attempts have been made to extend the validity region of both SPM and KA. Among these, the integral equation method [10] for extending the validity range of the high-frequency techniques should be mentioned. The scattering solution based on the integral equation method is obtained in [10] by inserting the KA-solution into the surface field integral equation. This method is significant in that it reduces the formalism to the SPM solution, thereby seemingly bridging the gap between the low and high frequency solutions.

Another group of analytical models is based on a description of the random surface as composite (two-scale) surface. It may occur that long-scale features of the real sea surfaces show significant influence on the total bistatic cross section. To account for these backscattering effects, Valenzuela [11] generalized the earlier results of Wright [12] to predict the total radar cross section from a small patch that is tilted in a specific manner. Wright referred to this model as the composite or the two-scale model. Different versions of this approach have widely been used by many researchers, especially in the field of ocean remote sensing. This approach has been used, for example, in [13]. However, the radar return from large- and small-scale surfaces is usually modeled in the frame of Physical Optics and Bragg scattering theories, respectively, as has been carried out in [14]. Such a model is, however, not general and does not describe all practical cases.

In radar imaging of the ocean surface, a modulation of the radar backscatter cross section by surface and internal waves determine the image characteristics [15]. In the past, the radar cross section modulation has been determined by using a just slightly rough model [16, 17]. However, this model does not include the effects of intermediate waves. At higher radar frequencies, the intermediate waves play a larger role in the modulation process. The slightly rough model is hence inadequate for predicting some of the experimentally observed modulation features in this case.

More recently, it has been shown in [18] that the Kirchhoff technique presented in [19] and the composite surface model are equivalent. In Ref. [20], the Kirchhoff method and the composite surface model are compared to each other with the central objective to show the equivalence of the two methods in low and moderate sea states and more importantly, to find limits of the composite surface

model in higher sea states.

In works [21, 22], the composite model has been extended to the more general bistatic problem. The Kirchhoff method has been used as a base, and the assimilation of large-scale tilting has been provided. In this approach, the scale separation should rather be determined by the characteristics of the scattering surface. This model includes, however, linear and small tilting only.

On the other hand, the effect of the internal waves on the capillary wave fields may result in a phase modulation of the latter. It is rather difficult to take this effect into account in the framework of the above-mentioned two-scale model. To consider the influence of different surface modulations of the scattering, it is necessary to use a more general theory.

In this paper, an approach for a description of the composite random rough surface is developed in order to have some progress in the solution of this problem. The basis for the analysis is an approximate solution of the integral equation, which describes the scattering from surfaces with small or moderate slopes [10]. Unlike the small perturbation theory developed in [11, 23], the surface height fluctuations do not appear as coefficients in the expressions for the diffuse scattered fields. Rather they appear in the phase term. Thus this solution is not restricted by the small surface height assumption.

Contrary to our previous paper [24], we consider here the case that the size of the illuminated surface is sufficiently large what allows us to use analytical averaging for both the small- and large-scale roughness. Since the amplitude of the statistically homogeneous small-scale component of the sea surface may be modulated by the large-scale components of the surface waves, a statistically inhomogeneous surface may appear. In order to take into account this effect and to increase the range of the wave solutions, the large-scale roughness is described in terms of Physical Optics theory. The developed approach allows us to investigate the strong reduction of the surface roughness which appears when oil films are on sea. Besides, this approach is more convenient to describe the scattering from rough surfaces for short electromagnetic waves used in remote sensing.

The emphasis in the numerical study is on the behavior of radar cross section and radar contrast, including spectral contrast, as a function of the backscattering angle. To apply the obtained results to real experimental situations which arise when the scattering from sea with and without an oil film is observed, the dependencies from different parameters of the inhomogeneous rough surface are studied. We also consider possibilities arising when two-frequency radar probing is provided. Finally, the obtained results are discussed from the point

of view of the explanation of experimental data.

2. THEORETICAL BACKGROUND

Consider electromagnetic wave scattering from a perfectly conducting random rough surface. Assume that a large surface wave with some random parameters modulates this surface. Here we consider only the case when both incident and scattered waves show horizontal polarization which is typical, for example, for satellite-based SAR.

The electric and magnetic fields inside a closed surface may be determined by the Stratton-Chu integral equations [25] which are a set of coupled equations that may be solved for appropriate boundary conditions. For perfect conductors, this set is decoupled. A full-wave technique following the KA has been developed in [26–28] and examined for the magnetic induction. A similar approach for the electric field has been used in [29].

In line with [29], the first term of the solution of the integral equation for the electric field shows the form

$$E = \frac{ik_z e^{i\vec{k}\vec{R}_a}}{4\pi|\vec{R}_a|} \int dx e^{-i\chi_x x - i\chi_z \zeta(x)}. \tag{1}$$

Here $|\vec{R}_a|$ means distance between a point at the surface and the observation point, $\chi_x = |\vec{k}|(\sin\theta_i - \sin\theta_s)$, $\chi_z = |\vec{k}|(\cos\theta_i + \cos\theta_s)$, $k_z = |\vec{k}|\cos\theta_i$ where θ_i and θ_s are the incidence and scattering angles, respectively, $\vec{k}$ is the wave vector of the incident wave, and $\zeta(x)$ means surface height at the horizontal position x.

Then for the intensity of the scattered electromagnetic field, one can readily write

$$I \sim \iint dx dx' e^{-i\chi_x(x-x') - i\chi_z[\overline{M}(x) - \overline{M}(x')] - i\chi_z[\widetilde{M}(x) - \widetilde{M}(x')]}. \tag{2}$$

Here $\overline{M}(x)$ is the mean part of the large-scale roughness, and $\widetilde{M}(x) = \xi_1(x) + \xi_2(x)$ where $\xi_1(x)$ and $\xi_2(x)$ mean height of the small- and large-scale roughness, respectively. Note that (2) does not contain any assumption regarding the surface statistics.

The next step is to develop a model describing the surface roughness. The amplitudes of the statistically homogeneous small-scale components of the sea surface may be modulated by the large-scale components of the surface waves. As a result, a statistically inhomogeneous surface appears. We consider the mathematical model describing this case.

Let $\xi_1(x)$ be a statistically homogeneous random field with correlation length l_1, and $\xi_2(x)$ a modulating function with a scale $l_2 \gg l_1$. In the most important applications, the function ξ_2 is close to periodic. Hence we can choose its mean part as $\overline{M}(x) = A\cos Kx$ (A, K are amplitude and wave number of the large surface wave, respectively). The function ξ_2 may contain some random parameters. For simplicity we assume that ξ_1 and ξ_2 are statistically independent.

For averaging we note that according to [30, 31], one can write for normally distributed random variables ξ_k

$$\left\langle \exp\left\{ i \sum_{k=1}^{n} q_k \xi_k \right\} \right\rangle = \exp\left\{ -\frac{1}{2} \sum_{r,s=1}^{n} W(\xi_r, \xi_s) q_r q_s \right\} \tag{3}$$

where $W(\xi_r, \xi_s) = \langle \xi_r \xi_s \rangle$.

We introduce new variables of integration $u = x - x'$ and $v = x + x'$, substitute them into (2), and average analytically by using (3). As result we obtain

$$\bar{I} \sim \int_{-L}^{L} dv \int_{-\infty}^{\infty} du\, e^{-i\chi_x u + 2i\chi_z A \sin(kv/2)\sin(ku/2)}$$
$$\cdot\, e^{-\chi_z^2 [<h_1^2>(1-R_1) + <h_2^2>(1-R_2)]}. \tag{4}$$

Here $2L$ is the linear size of the illuminated area, R_1, R_2 are the correlation functions, and $h_1^2 = <\xi_1^2>$, $h_2^2 = <\xi_2^2>$ mean rms height of the small- and large-scale roughness, respectively.

Consider the case of a Gaussian probability distribution of both the small- and large-scale components of the surface waves. Such description of the roughness allows us to study the influence of the different ranges of the spatial spectrum on the scattering process. It is worth noting that one can use another probability density of the spectrum, say, a Pierson-Moscowitz spectrum, in the framework of this model.

In order to simplify Eqn. (4), we expand the term taking into account the large-scale roughness into a Taylor series up to the second term. As a result, we obtain instead of (4)

$$\bar{I} \sim e^{-\chi_z^2 <h_1^2>} \int_{-L}^{L} dv \int_{-\infty}^{\infty} du\, e^{-i\chi_x u + 2i\chi_z A \sin(Kv/2)\sin(Ku/2)}$$
$$\cdot\, e^{\chi_z^2 [<h_1^2>e^{-u^2/L_1^2} + <h_2^2>(u/L_2)^2]}. \tag{5}$$

Expanding the integrand of (5) into an infinite Taylor series and evaluating the corresponding integrals by the Laplace method, we

obtain the following expression for the radar scattering cross section:

$$\sigma = \sqrt{\pi} L\, e^{-\chi_z^2 h_1^2} \sum_{m=0}^{\infty} \frac{1}{m!} (\chi_z h_1)^{2m} S_0^{-1/2} \sum_{r=0}^{\infty} (\chi_z A/2)^{2r} \Phi(r) T(r) \quad (6)$$

where

$$\Phi(r) = \frac{1}{(r!)^2} + 2(-1)^r \sum_{n=0}^{r-1} \frac{(-1)^k}{n!(2r-n)!} \sin c[KL(r-n)],$$

$$S_0 = \chi_z^2 \frac{h_2^2}{l_2^2} + \frac{m}{2l_1^2},$$

$$T(r) = \sum_{s=0}^{2r} \frac{(-1)^s (2r)!}{s!(2r-s)!} e^{-[\chi_x - K(r-s)]^2/(4S_0)}.$$

Eqn. (6) describes the scattering process for a broad class of random surfaces and gives us a possibility to consider realistic cases of variations in the spectrum of surface waves observed for a sea surface with and without oil films.

When the short-wave range of the electromagnetic waves is used for remote sensing of the sea surface, it is possible to simplify (6) by taking into account that the inequality $|r - s|K \ll \chi_x$ holds for a wide range of variations of r and s, except for the small range near vertical incidence. Besides, we suppose that $\chi_x K/(\chi_z \gamma)^2 \ll 1$ where $\gamma = h_2/l_2$ is the slope of the large-scale roughness. Then one can write the expression for the radar scattering cross section as

$$\sigma = \sqrt{\pi} L\, e^{-\chi_z^2 h_1^2} \sum_{m=0}^{\infty} \frac{1}{m!} (\chi_z h_1)^{2m} S_0^{-1/2} e^{-\chi_x^2/(4S_0)} M(m) \quad (7)$$

where

$$M(m) = \sum_{r=0}^{\infty} [\chi_x \chi_z AK/(4s_0)]^{2r} e^{-\chi_x K r/(4S_0)} \Phi(r).$$

If $KL = m_1 \pi$, $m_1 = 1, 2, \ldots$, the following identity can be used to simplify (7):

$$M(m) = J_0(y) \quad (8)$$

where $J_0(y)$ is the Besssel function of zeroth order, whose argument is given by $y(m) = i\chi_x \chi_z AK \exp[-\chi_x K/(4S_0)]/(2S_0)$. Note that for the cases of most practical importance, the value of KL is usually so large that the second term in the above expression for $\Phi(r)$ (sum over n) is negligibly small as compared to the first one. Then one can use (7) with $M(m)$ given by (8) even if $KL \neq m_1 \pi$.

3. NUMERICAL RESULTS

The expression (7) allow us to investigate how the different ranges of the spectrum of the surface waves influence the scattering process. To demonstrate such effects, we have carried through extensive numerical simulations by using expressions (7) and (8) for the case of backscattering of a radar signal applied by a remote sensing system. A term $\sqrt{\pi} L\, e^{-(\chi_z h_1)^2}/\chi_z$ in (7) is omitted when calculating the scattering cross section.

Firstly, consider the changes in the backscatter signal caused by variations of the small-scale roughness. We assume that there is a large-scale roughness with a tangent of the angle of its slope (γ) equal to 0.1. In Fig. 1(a), the radar scattering cross section is shown as a function of incidence angle for a correlation length which is equal to 0.43λ at two different values of the rms height, what corresponds to curves 1 and 2. Fig. 1(b) presents the same angular dependencies at different correlation lengths for a small rms height which is equal to 0.042λ. As can be seen, a variation of the small-scale roughness results in a strong (about 10–15 dB) change in the scattered intensity.

A comparison between scattering from a surface with small roughness and a two-scale (large and small roughness) random surface has also been drawn. The results are presented in Figs. 1(c), (d). In this case, the correlation lengths are 0.046λ and 0.43λ for Figs. 1(c) and 1(d), respectively. The dashed and solid curves are related to small and large plus small scales of roughness, respectively. γ is equal to 0.32. It can be seen that a modulation of the scattered signal which is due to the effect of the large-scale roughness can be observed at near-vertical angles of incidence for the case of a small correlation length. However, if the correlation length shows a moderate value, a maximum in the increase of the backscatter signal is observed at intermediate incidence angles. For both cases, this effect is more pronounced for small values of the rms height than for moderate ones.

When the oil film damps the sea waves, both the rms height and the correlation length can be reduced simultaneously. Examples of the angular behavior of the cross section are given in Fig. 2. Fig. 2(a) corresponds to the case when both rms height and correlation length are varied and the surface shows only small-range roughness. It is seen that the cross section can be decreased by up to 15–20 dB at intermediate incidence angles.

According to the present understanding, the damping effect of the oil film leads to an attenuation of the spectral power over the whole range of the spectrum [5]. Hence it is interesting to discuss how the presence of a long surface wave will influence the value of
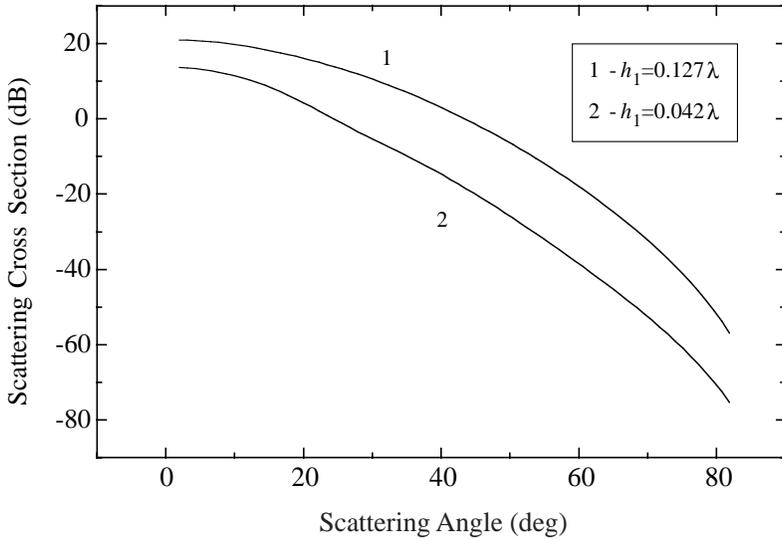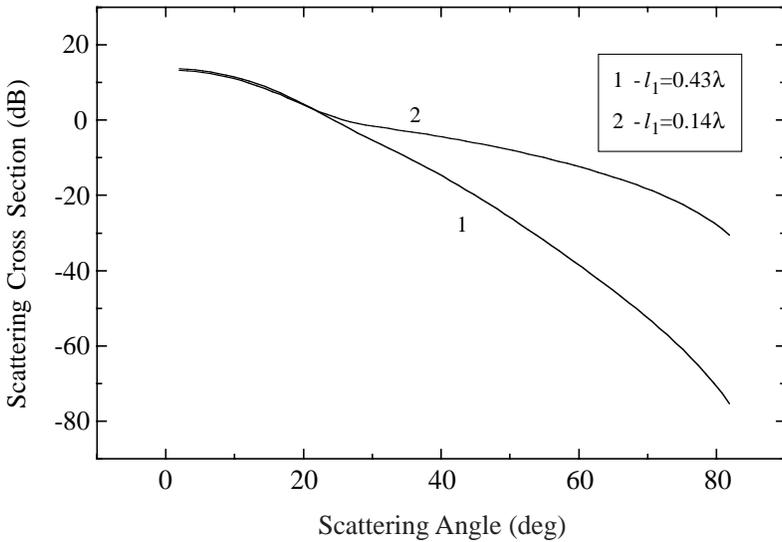
Figure 1. Scattering cross section versus scattering angle: (a) for different rms heights at $l_1 = 0.43\lambda$; (b) for different correlation lengths at $h_1 = 0.042\lambda$. The large-scale components are given by $\gamma^2 = 0.01$, $AK = 0.1$, $K = 2\pi/\Lambda$, $\Lambda = 1\,\mathrm{m}$, $k/K = 3 \cdot 10^3$.
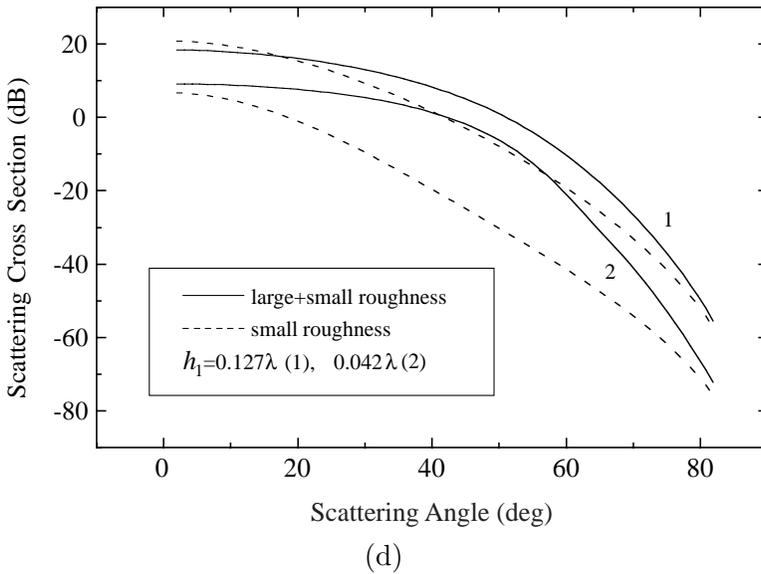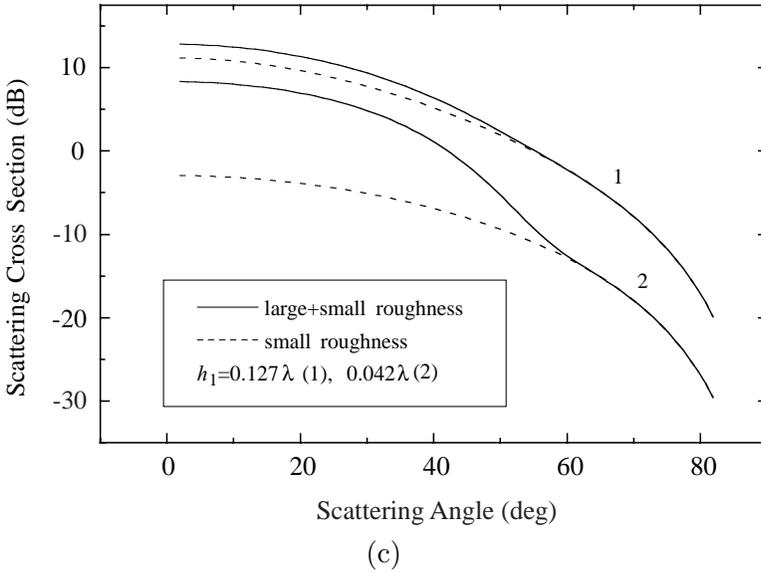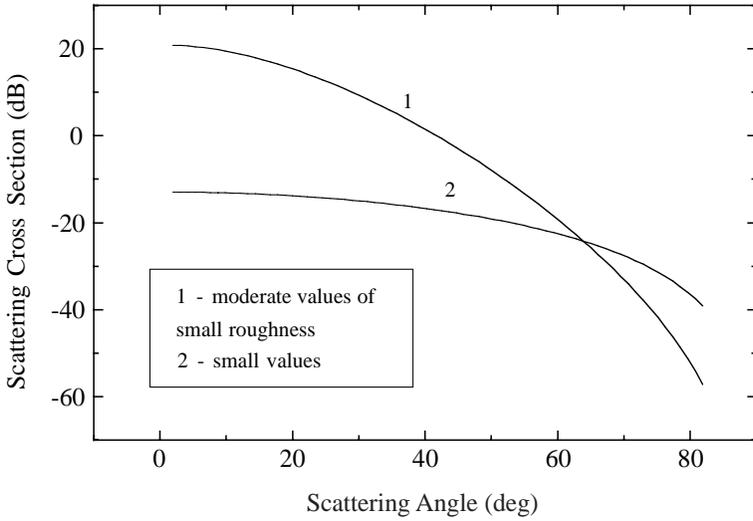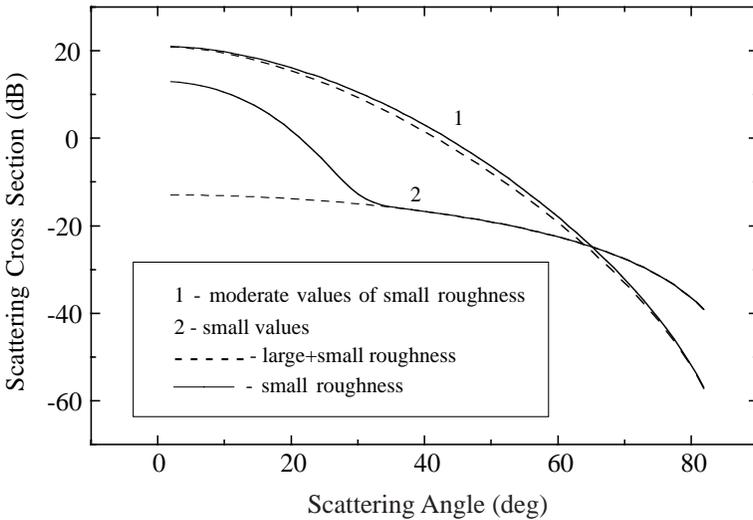
(c)

(d)

Figure 1. (cont'd) Scattering cross section versus scattering angle: (c) comparison between the cases of large plus small and only small roughness at different rms heights and $l_1 = 0.046\lambda$; (d) the same as (c) at $l_1 = 0.43\lambda$. The large-scale components are given by $\gamma^2 = 0.1$, $AK = 0.1$, $K = 2\pi/\Lambda$, $\Lambda = 1\,\text{m}$, $k/K = 3 \cdot 10^3$.

Figure 2. Scattering cross section as a function of scattering angle for moderate and small values of small roughness: (a) 1 - $h_1 = 0.127\lambda$ and $l_1 = 0.43\lambda$, 2 - $h_1 = 0.014\lambda$ and $l_1 = 0.046\lambda$; (b) the same together with results obtained for the case of large plus small roughness; parameters of large-scale components: $\gamma^2 = 0.01$, $AK = 0.1$, $K = 2\pi/\Lambda$, $\Lambda = 1\,\text{m}$, $k/K = 3 \cdot 10^3$.

the radar scattering cross section. Fig. 2(b) illustrates the results of backscattering for different average slopes of long surface waves when the rms height of the small-scale roughness shows small and moderate values. Here the radar scattering cross section from surfaces with rms heights equal to 0.127λ and 0.014λ and correlation lengths equal to 0.43λ and 0.046λ is presented as curves 1 and 2, respectively. The variation of the slope value can correspond to backscattering from slick and sea in a special experimental situation. As can be seen from Fig. 2(b), there is a certain range of incidence angles (in this example, it extends from 20 up to 40 degrees) where changes of the roughness parameters exert the strongest effect on the value of the radar scattering cross section.

As is known, dark and brighter areas are observed in the radar images. They correspond to slick-covered and slick-free areas of the sea surface. For an adequate interpretation of the backscattering from these surfaces, it is more convenient to introduce the radar contrast K_r as the ratio of two backscatter cross sections from two random surfaces with different parameters. Throughout this paper, the contrast K_r is defined as the ratio of the radar scattering cross section for the surface with larger roughness to that for the surface with smaller roughness.

Let us now consider how the parameters of a two-scale random surface change the value of K_r. First of all, we investigate the influence of the small-scale roughness. Fig. 3(a) shows K_r as function of the incidence angle. In this case, $h_{11} = 0.046\lambda$ and l_{11} (which is varied) describe the random surface with smaller roughness while $h_{12} = 0.127\lambda$ and $l_{12} = 0.24\lambda$ are related to the random surface with larger roughness.

Usually the theoretical study of electromagnetic scattering from a rough surface is illustrated by curves which show the dependencies of the scattering cross section or/and of the mean field on the scattering angle. However, often in radar images, the area with an oil film is so small that the range of scattering angles for the backscatter signal from the oil-slick covered surface is not significant. In this case, the traditional angular dependencies become insufficient. Therefore we consider K_r as a function of the average slope of the short-range spectrum of roughness for several values of the backscattering angle. The results are presented in Fig. 3(b). The curves 1, 2, 3 are related to angles of 30, 45, and 60 degrees, respectively. It appears that at large angles ($\sim$ 60 degrees), there is a depression in the backscatter signal (for a range of the slope of 0.15 to 0.32) which is caused by a decreasing value of the slope for the surface with smaller roughness (curve 3). However, if the incidence angle is in the range of 30–40 degrees, the contrast is just weakly sensitive to the variation of the
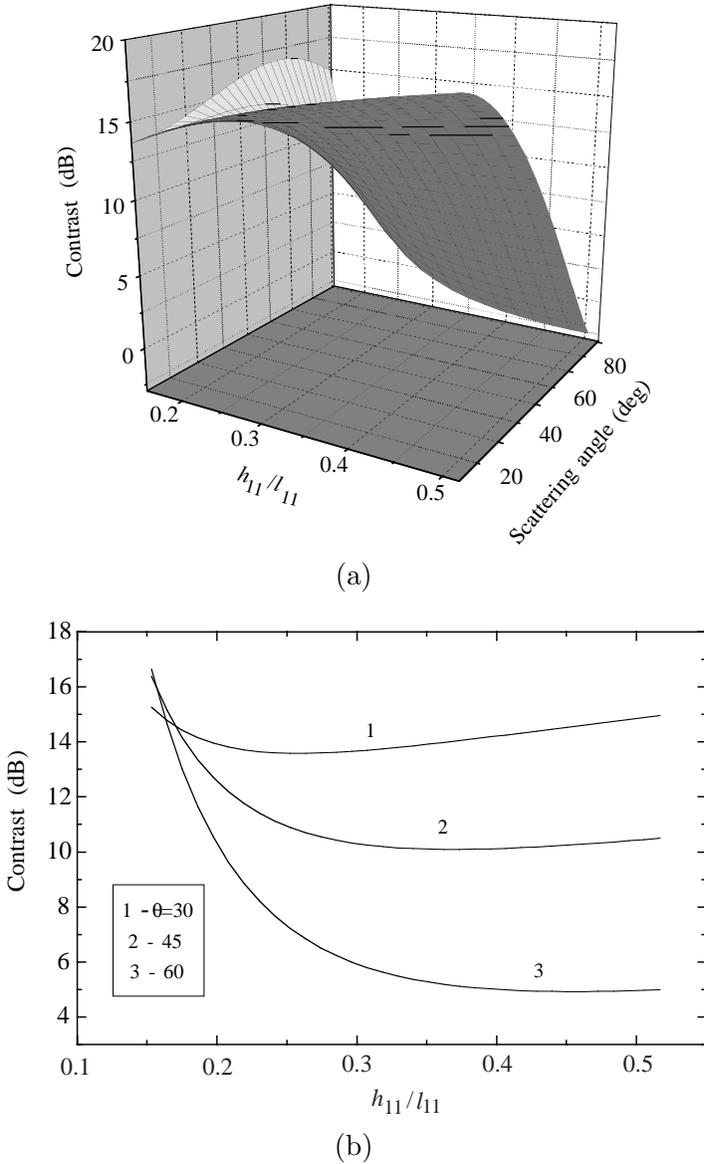
(a)

(b)

Figure 3. Contrast as a function of small-scale roughness: (a) angular behavior of contrast with varying angle of slope for small-scale roughness (h_{11}/l_{11}); (b) contrast as a function of slope for several values of scattering angle. First (smoother) surface: $h_{11} = 0.042\lambda$, l_{11} is varied; second surface: $h_{12} = 0.127\lambda$ and $l_{12} = 0.24\lambda$. No long wavelength waves are taken into account.
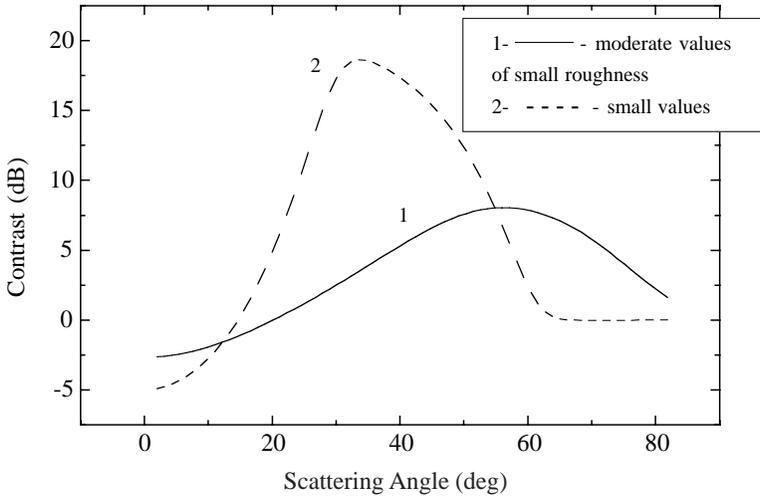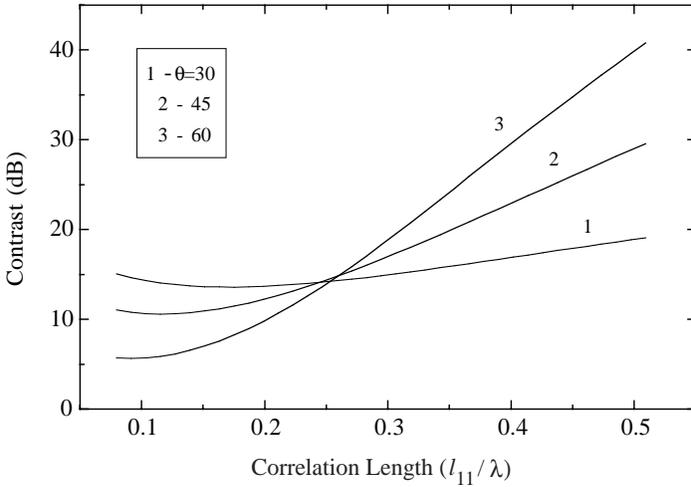
Figure 4. Contrast as a function of scattering angle. Curve 1 has been calculated for moderate values of small-scale roughness ($h_1 = 0.127\lambda$, $l_1 = 0.43\lambda$) and slope of the large-scale roughness $\gamma_1^2 = 0.01$. Curve 2 has been calculated for small values of the small-scale roughness ($h_1 = 0.014\lambda$, $l_1 = 0.046\lambda$) and slope of the large-scale roughness $\gamma_1^2 = 0.1$. The mean part of large surface waves is the same as in Fig. 1.

slopes of a random surface. Note that in the latter case, the significant value of the contrast ($\sim 14\,\text{dB}$) can be caused by a significant difference in the values of h and l for the two random surfaces.

Now we consider how the change of parameters of long waves of the surface spectrum influences the contrast. Figure 4 shows K_r as function of the incidence angle for moderate (curve 1) and small (2) roughness of the small-scale spectrum. In our case, K_r means the ratio between the backscatter cross sections for two surfaces which have a small roughness, as is indicated above, and a large-scale roughness with $\gamma = 0.32$ (curve 1) and 0.1 (2). It is seen that K_r can reach values up to $20\,\text{dB}$ depending on the slope value. The shift of the peaks occurs because the values of the parameters of the small-scale roughness are increased. Note that experimental curves for K_r obtained at C- and Ku-band show that the depression in backscattering can be about $10\,\text{dB}$ and higher [2].

Consider next how the long wave spectral portion influences the contrast. The situation which is illustrated by Figs. 5(a), (b) corresponds to the case that the surface with larger roughness shows

(a)
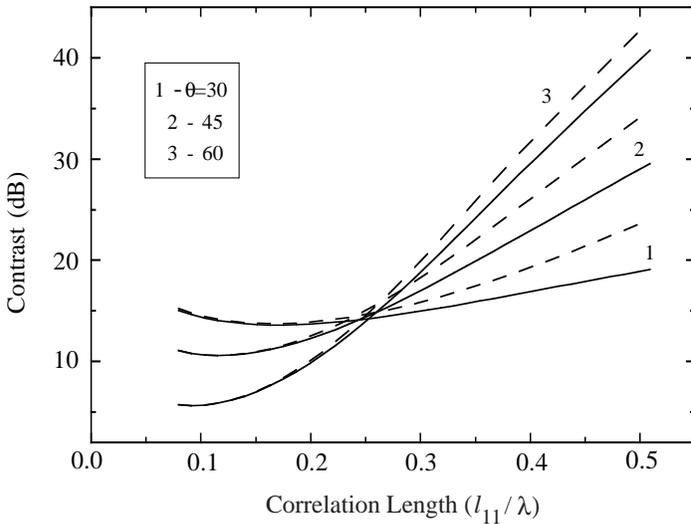
(b)

Figure 5. Contrast as a function of the correlation length of small-scale roughness for several values of the scattering angle: (a) $h_{11} = 0.042\lambda$, l_{11} is varied for the first surface, and $h_{12} = 0.127\lambda$ and $l_{12} = 0.24\lambda$ for the second one, $\gamma_1^2 = \gamma_2^2 = 0.01$; (b) the same curves as in case (a) (solid curves) plus contrast obtained for the case with $\gamma_1 = 0$ and the same other parameters as in case (a) (dashed curves). The mean part of the large-scale roughness is the same as in Fig. 1.

fixed values of h and l, the surface with smaller roughness shows a varying l-value and hence a varying slope of the small-scale roughness (high-frequency part of the roughness spectrum), while the slope of the large-scale roughness (low-frequency part) is equal for both surfaces and kept constant. It is apparent that the depression in the backscattering due to the reduced correlation length can reach considerably large values as can be seen from Fig. 5(a).

In Fig. 5(b), similar studies are provided for the case that $\gamma_1^2 = 0$ and $\gamma_2^2 = 0.01$ for the surfaces with smaller and larger values of the high-frequency part of the spatial spectrum, respectively. For comparison, the curves from Fig. 5(a) are also presented. It is obvious that the curves in Figs. 5(a) and 5(b) show very similar behavior. This fact confirms that the direct influence of the large-scale roughness on the backscattering intensity is insignificant.

Variations in the correlation length and rms height can lead to a depression of the signal scattered from a smooth surface. Fig. 6(a) shows K_r versus the scattering angle for various correlation lengths of the smooth surface ($\gamma_1^2 = 0.01$). For the surface with larger values of the roughness, all parameters are held constant: $l_2 = 0.24\lambda$, $\gamma_2^2 = 0.1$. The value of the rms height is equal to 0.042λ for both surfaces.

Results for comparing the contrast for the two cases that the rms height shows values of 0.042λ and 0.127λ are presented in Fig. 6(b). The other parameters characterizing the roughness of the surfaces are the same as those in the example shown in Fig. 6(a). Again, as in Fig. 5, the depression in the backscattering caused by the small-scale roughness is considerably large (the contrast is changed up to 20–30 dB). However, a significant decrease of the contrast is observed for higher rms height. (K_r is about 0–3 dB for $h_1 = 0.127\lambda$ at a backscattering angle of $\theta = 30$ degrees).

Furthermore, the stronger dependencies are observed for larger angles of scattering. This effect illustrates the well-known fact that the scattering from the long-wave components of the spatial spectrum is stronger for scattering angles close to nadir, while at intermediate angles the small roughness plays the main role in the scattering process, and the contrast then varies rapidly for all parameters of the small-scale roughness.

Finally, to investigate the dependencies of the backscattering over the whole range of the spatial spectrum of the random surface, we consider the contrast behavior at average angles of the slope of long waves. The results are presented in Figs. 7(a), (b). Again, two random surfaces are assumed showing moderate and small values of the high-frequency part of their spatial spectrum, and the smoother surface is characterized by its slope angle which is varied. A more rapid decrease
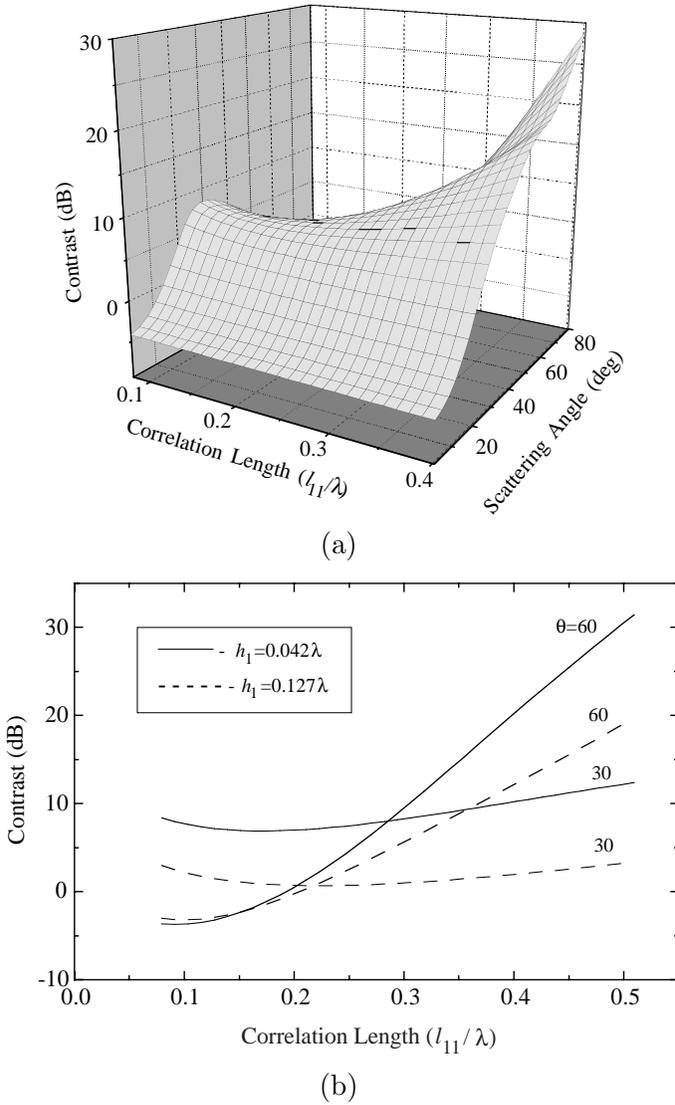
(a)

(b)

Figure 6. Contrast behavior for different rms heights of the small-scale roughness: (a) contrast as a function of the normalized correlation length (l_{11}/λ) and of the scattering angle; $h_1 = h_{11} = h_{12} = 0.042\lambda$, l_{11} is varied, $l_{12} = 0.24\lambda$, $\gamma_1^2 = 0.01$, $\gamma_2^2 = 0.1$; (b) contrast as a function of l_{11}/λ for two rms heights of small-scale roughness: $h_1 = 0.042\lambda$ (solid curves), $h_1 = 0.127\lambda$ (dashed curves). The other parameters are the same as in case (a). The scattering angles are $\theta = 30$ and 60 degrees. The mean part of the large-scale roughness is the same as in Fig. 1.
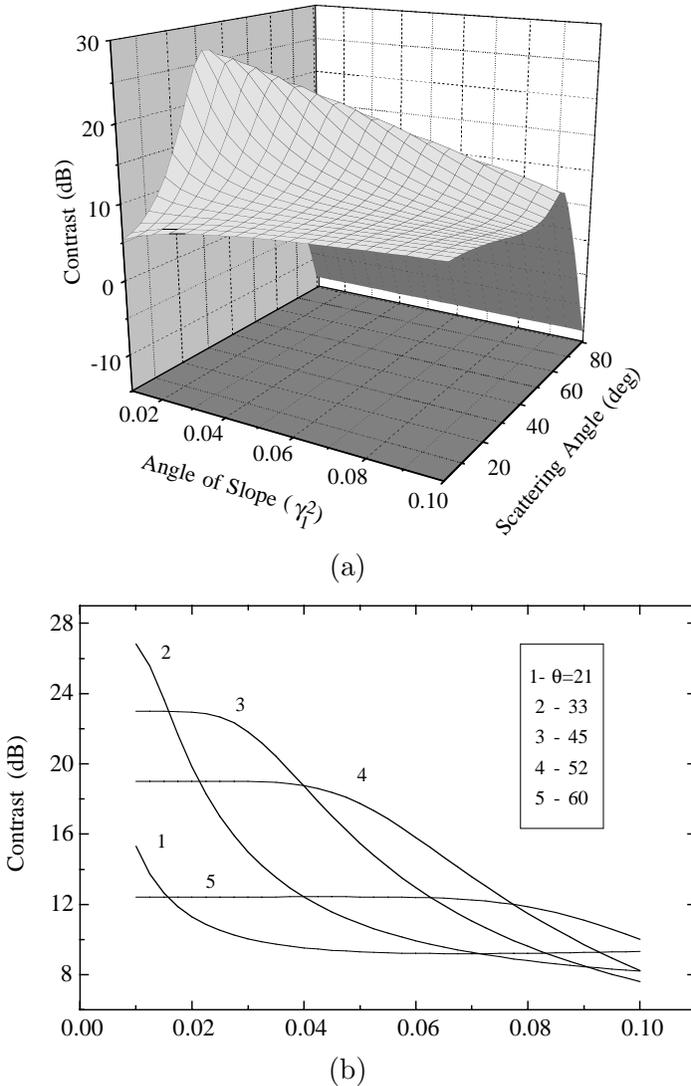
(a)

(b)

Figure 7. Behavior of contrast depending on the slope angle for large-scale roughness: (a) contrast as a function of the angle of the slope of large-scale roughness and of the scattering angle; $h_{11} = 0.014\lambda$, $l_{11} = 0.046\lambda$, $h_{12} = 0.127\lambda$, $l_{12} = 0.43\lambda$, $\gamma_2^2 = 0.1$; (b) contrast as a function of γ_1^2 at several values of the scattering angle θ shown in degrees at the same parameters as in case (a). The mean part of the large-scale roughness is the same as in Fig. 1.
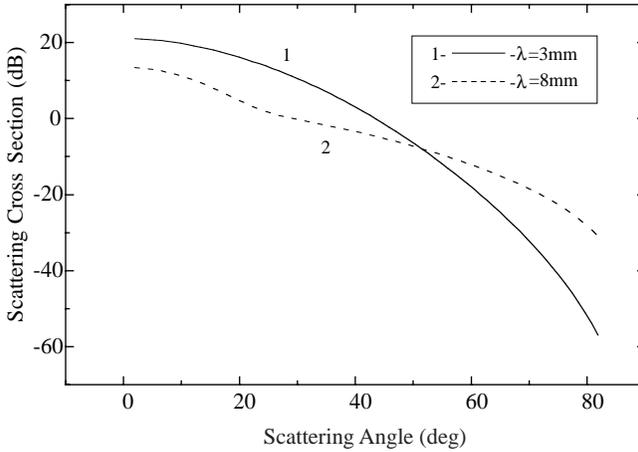
Figure 8. Angular behavior of the scattering cross section for different wavelengths of the incident field: $h_1 = 0.127\lambda_{\min}$, $l_1 = 0.43\lambda_{\min}$, $\gamma^2 = 0.1$. The mean part of the large-scale roughness is the same as in Fig. 1.

of the scattering is observed at intermediate incidence angles. It is also apparent that the larger angle of the slope leads to small changes of the backscattering over the whole range of incidence angles (see the range near $\gamma^2 = 0.1$ in Fig. 7(b)). In general, such behavior of the contrast occurs due to the presence of a small roughness which is modulated by the large-scale components.

It is interesting to investigate which additional possibility could appear if two electromagnetic waves with different frequencies are used for remote sensing of sea surface and oil films. Fig. 8 illustrates the difference between the scattering radar cross sections for waves with $\lambda = 3$ mm and 8 mm while the characteristics of the rough surface show fixed parameters. It is supposed that the condition $k/K = 3 \cdot 10^3$ is kept when $\lambda = 3$ mm. The variation in the backscattering due to the frequency change is similar to that due to the change of the random surface parameters. Hence this fact can be used to determine which part of the spatial spectrum is responsible for the reduction of the radar signal scattered from oil slick. This should be important for distinguishing between signals backscattered from an oil film and from other smoothing areas of the sea surface.

For a more convenient description of the experiment with two frequencies of the incident waves, we introduce a spectral contrast, K_s, determined as the ratio of the contrasts for the two electromagnetic waves. An example of the angular behavior of K_s is given in Fig. 9.
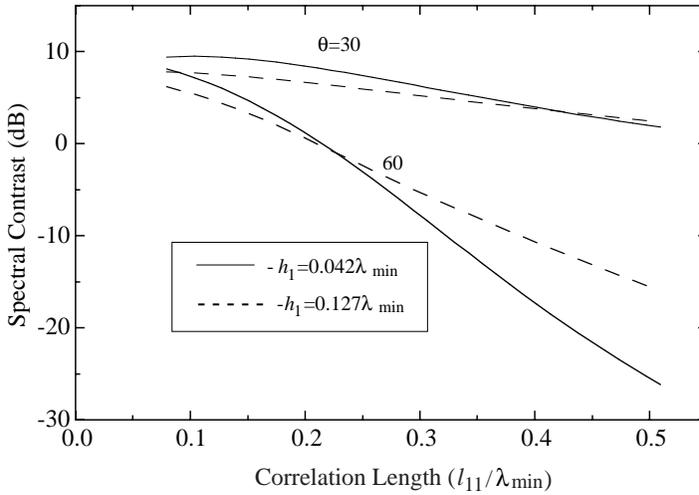
Figure 9. Spectral contrast depending on correlation length of the small-scale roughness for electromagnetic waves with $\lambda = 8$ mm and $\lambda = 3$ mm. The radar contrasts for both wavelengths are obtained in the same manner and at the same parameters of the surface as in Fig. 6(a). The spectral contrast as a function of l_{11}/λ_{min} is shown for two values of the rms height: $h_1 = 0.042\lambda_{min}$ (solid curves), $h_1 = 0.127\lambda_{min}$ (dashed curves) at $l_{12} = 0.24\lambda_{min}$, $\gamma_1^2 = 0.01$, and $\gamma_2^2 = 0.1$. The scattering angles are $\theta = 30$ and 60 degrees. The mean part of the large-scale roughness is the same as in Fig. 1.

Here K_s presents the ratio of the contrasts K_r for incident waves with wavelengths of 8 mm and of 3 mm, i.e., $K_s = K_r(\lambda = 8\,\text{mm})/K_r(\lambda = 3\,\text{mm})$. The scattering random surfaces show parameters covering the whole range of roughness. As is seen in Fig. 9(b), a stronger dependence of K_s on the correlation length is observed for large incidence angles (curves 2 and 3). A comparison of the spectral contrasts obtained for two different rms heights also yields a stronger dependence at large incidence angles. The observed phenomena can be used for determining the values of the roughness parameters.

The same spectral contrast as a function of the angle of the slope of long waves is displayed in Fig. 10. It appears that similar as in the above examples, the spectral contrast dependencies of scattering from large-scale components are weaker than those of scattering from small-scale components. It is interesting to note that different ranges of the incidence angle correspond to different ranges of the slope angle where the spectral contrast varies most rapidly.
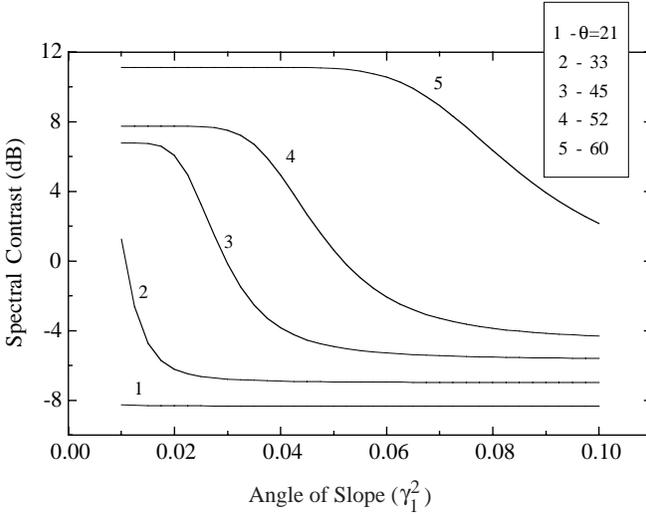
Figure 10. Spectral contrast as a function of the slope of the large-scale roughness. The contrasts for both wavelengths are obtained in the same manner and at the same parameters of the surface as in Fig. 7(a). The spectral contrast as a function of γ_1^2 is shown at several values of the scattering angle θ, at $h_{11} = 0.014\lambda_{\min}$, $l_{11} = 0.046\lambda_{\min}$, $h_{12} = 0.127\lambda_{\min}$, $l_{12} = 0.43\lambda_{\min}$, $\gamma_2^2 = 0.1$. The mean part of the large-scale roughness is the same as in Fig. 1.

4. DISCUSSION AND CONCLUSIONS

To summarize, we discuss some results obtained in the framework of the developed composite surface model from the viewpoint of remote sensing for detecting the oil films and distinguishing them among look-alike areas. Firstly, indicate that in the general case the sea surface may be inhomogeneous because of the modulation of the statistically homogeneous small-scale components by the large-scale part of the spectrum. This can correspond to swell or internal waves [32]. Hence a model of the surface must include the term, which is responsible for this effect. In our work an attempt has been made to do this. In the most interesting cases, the inhomogeneous part will be close to periodic or near periodic, if it is caused by the joint effects of wind and gravity waves on capillary waves. Hence the mean part of the modulating inhomogeneous part is described by a cosine function as has been suggested in [32]. Note that most of the numerical results show a significant influence of the modulation effect on the behavior of the scattering process.

It should be noted that a description of the statistically homogeneous part (the small-scale roughness) which extends the range of validity beyond the usually used small-perturbation theory, allows us to study the scattering when the parameters of roughness are of the same order as the electromagnetic wavelength. Hence using such a model provides a correct interpretation of the scattering process while the spatial spectrum varies over a broad range because of the damping effect which is caused by the oil slick covering the sea surface.

We discuss now the angular behavior of the radar scattering cross-section. The model developed in this paper allows to obtain the angular characteristics for the depression of the backscattering which are similar to the experimental curves which have been shown in [2]. Note that such an angular behavior in the backscatter depression is possible only if the short-wave range of the roughness spectrum is modulated by long-length wave components. If they are absent, the modulation is of another kind. Note further that the strong effect of the large-scale roughness on the scattering process can also be seen in Figs. 1(c), (d), and 2. The effect extends also to the mid-angle range. Hence it is necessary to take this phenomenon into account in order to explain the experimental data from a SAR or side-looking radar.

Since a discrimination of the various types of the depression of the ocean spectrum is one of the main aims of remote sensing of oil films, it is necessary to study the influence of the different ranges of the spectrum. The numerical study shows that both short and long wave ranges can decrease the backscatter power. The value of this depression can reach 15–20 dB when the amplitude of the mean part of the long waves varies from 0.1 to 0.5 of the wavelength or when the γ-value is decreased from 0.32 to 0.1. The observed experimental remote sensing data can thus be explained in the frame of this large-scale variation.

The area covered by an oil film may show but a small size which is unknown a priori. The angular width of such a spot in the images, which are obtained by an airborne or spaceborne radar, can be insufficiently large to study the angular behavior of backscattering. For such cases, we consider the depression in backscattering as a function of the different parameters over the whole roughness spectrum while the scattering angle has a constant value.

The numerical results for the contrast can well be compared with experimental data. The ratio between the backscattering signals, which is introduced by the definition of the spectral contrast, may mean the ratio between the scattering from the sea surface surrounding the oil spot to that from the oil film area. It should be noted that in the real experimental situation, the values of the contrast may be smaller. This fact is connected with reducing the contrast if the slope of long

wave components is increased.

The main characteristics of the contrast behavior over the whole range of observation are the following. The most significant dependencies are observed for higher angles of incidence (at the end of the mid-angle range). The changes in the values of the small-scale roughness cause a stronger influence on the backscatter signal. However, if the slope angle of the large-scale components is increased, the variation in backscattering depending on small-scale components is decreased.

Additional possibilities have appeared if one uses two-frequency probing of the oil slick surface and surrounding sea. We have studied the difference between the contrasts for scattering at two different electromagnetic wavelengths, $\lambda = 3\,\text{mm}$ and $8\,\text{mm}$. The angular characteristics for the radar cross section show the range of the scattering angles in which the difference between the scattered signals at the two frequencies is more significant. Again, this difference is stronger for large angles of incidence. As follows from the numerical results, it is possible to evaluate the parameters of the small-scale roughness from two-frequency experimental data since the difference between the contrasts can reach 5–10 dB. To summarize, the difference between the backscatter signals arising due to the influence of different ranges of the ocean spectrum can be useful for distinguishing between the scattering from surfaces of various types which smother the ocean.

REFERENCES

1. Alpers, W. and H. Huhnerfuss, "The damping of ocean waves by surface films: A new look at an old problem," *J. Geophys. Res.*, Vol. 94(C), 6251–6265, 1989.

2. Singh, K. P., A. L. Gray, R. K. Hawkins, and R. A. O'Neil, "The influence of surface oil on C-and Ku-band ocean backscatter," *IEEE Trans. Geosci. Rem. Sens.*, Vol. GE-24, 738–744, 1989.

3. Frate, F., A. Petrocchi, Lichtenegger, and G. Calabresi, "Neural network for oil spill detection using ERS-SAR data," *IEEE Trans. Geosci. Rem. Sens.*, Vol. GE-38, 2282–2288, 2000.

4. Solberg, A. H., Schistad, G. Storvik, R. Solberg, and E. Volden, "Automatic detection of oil spills in ERS SAR images," *IEEE Trans. Geosci. Rem. Sens.*, Vol. GE-37, 1916–1924, 1999.

5. Maclin, J. T., "The imaging of oil slicks by synthetic-aperture radar," *GEC Journal of Research*, Vol. 10, 19–28, 1992.

6. Rice, O., "Reflection of electromagnetic waves by slightly rough surfaces," *Commun. Pure Appl. Mathem.*, Vol. 4, 351–358, 1951.

7. Nieto-Vespirenas, M., "Depolarization of electromagnetic waves

scattered from slightly rough random surfaces: a study by means of the extinction theorem," *J. Opt. Soc. Am.*, Vol. 72, No. 5, 539–547, 1982.

8. Agarwal, G. S., "Interaction of electromagnetic waves at rough dielectric surface," *Phys. Rev. B*, Vol. 15, 2371–2383, 1977.

9. Beckmann, P. and A. Spizzichino, *The Scattering of Electromagnetic Waves from Rough Surfaces*, Pergamon, New York, 1963.

10. Fung, A. K., *Microwave Scattering and Emission Models and Their Applications*, Artech House, Norwood, MA, 1994.

11. Valenzuela, G. R., "Theories for the interaction of electromagnetic and oceanic waves — a review," *Boundary Layer Meteorol.*, Vol. 13, 61–85, 1978.

12. Wright, J. W., "A new model for sea clutter," *IEEE Trans. Antennas Propag.*, Vol. AP-16, 217–223, 1968.

13. Conway, J. A., R. A. Cordey, and J. T. Maclin, "Contrasts on two-scale descriptions of backscattering from the sea surface using scatterometer model functions," *Proc. IGARSS'88*, Edinburgh, ESA SP-284, 33–34, 1988.

14. Brown, G. S., "Backscattering from a Gaussian distributed perfectly conducting rough surface," *IEEE Trans. Antennas Propag.*, Vol. AP-26, 472–482, 1978.

15. Hasselmann, K., R. K. Raney, W. J. Plant, W. R. Alpers, R. A. Shuchman, D. R. Lyzenga, C. L. Rufenach, and M. J. Tucker, "Theory of synthetic aperture radar ocean imaging: A MARSEN view," *Journal of Geophysical Research*, Vol. 90, 4659–4686, 1985.

16. Alpers, W. R., D. B. Ross, and C. L. Rufenach, "On the detectability of ocean surface waves by real and synthetic aperture radar," *Journal of Geophysical Research*, Vol. 86, 6481–6498, 1981.

17. Wright, J. W., W. J. Plant, W. C. Keller, and W. L. Jones, "Ocean wave-radar modulation transfer functions from the West Coast Experiment," *Journal of Geophysical Research*, Vol. 85, 4957–4966, 1980.

18. Thompson, D. R., "Calculation of radar backscatter modulation from internal waves," *Journal of Geophysical Research*, Vol. 93, 12371–12380, 1988.

19. Holiday, D., G. St-Cyr, and N. E. Woods, "A radar imaging model for small to moderate incidence angles," *Int. J. Remote Sensing*, Vol. 7, 1809–1834, 1986.

20. Kasilingam, D. P. and O. H. Shemdin, "The validity of the composite surface model and its applications to the modulation of

radar backscatter," *Int. J. Remote Sensing*, Vol. 13, 2079–2104, 1992.

21. Elfouhaily, T., D. R. Thompson, B. Chapron, and D. Vanemark, "A new bistatic model for electromagnetic scattering from perfectly conducting random surfaces," *Waves Random Media*, Vol. 9, 281–294, 1999.

22. Elfouhaily, T., D. R. Thompson, B. Chapron, and D. Vanemark, "A new bistatic model for electromagnetic scattering from perfectly conducting random surfaces: numerical evaluation and comparison with SPM," *Waves Random Media*, Vol. 11, 33–43, 2001.

23. Ishimaru, A., *Wave Propagation and Scattering in Random Media*, Academic Press, New York, 1978.

24. Timchenko, A. I., A. E. Serebryannikov, and K. F. Schuenemann, "The influence of the finite size of the illuminated area on electromagnetic scattering from surfaces with and without slicks," *Progress in Electromagnetic Research*, Vol. 33, 237–259, 2001.

25. Stratton, J. A., *Electromagnetic Theory*, McGraw-Hill, New York, 1941.

26. Holiday, D., L. L. DeRaad Jr., and G. J. St-Cyr, "New equations for electromagnetic scattering by small perturbations of a perfectly conducting surface," *IEEE Trans. Antennas Propag.*, Vol. AP-46, 1427–1432, 1998.

27. Holiday, D., G. St-Cyr, and N. E. Woods, "Comparison of a new radar ocean imaging model with SARSEX internal wave image data," *Int. J. Remote Sensing*, Vol. 8, 1423–1430, 1987.

28. Holiday, D., "Resolution of controversy surrounding the Kirchhoff approach and the small perturbation method in rough surface scattering theory," *IEEE Trans. Antennas Propag.*, Vol. AP-35, 120–122, 1987.

29. Timchenko, A. and A. Tropina, "Subsurface detection and discrimination of buried objects group using remote sensing technique," *Proc. IGARSS'99*, Vol. 5, 2681–2684, 1999.

30. Rice, S., "Mathematical analysis of random noise," *Noise and Stochastic Processes*, N. Wax (ed.), Dover Publ., Inc., New York, 1954, 182.

31. Lynch, P. J., "Curvature corrections to rough-surface scattering at high-frequencies," *J. Acoust. Soc. Am.*, Vol. 47, 804–815, 1970.

32. Tatarskii, V. and S. F. Clifford, "On the theory of Dk radar observations of ocean surface waves," *IEEE Trans. Antennas Propagat.*, Vol. AP-43, 843–850, 1995.